

1-1-93  
E7414

NASA Technical Memorandum 105921

# Processing and Microstructure of Nb-1%Zr-0.1%C Alloy Sheet

Mehmet Uz  
*Lafayette College*  
*Easton, Pennsylvania*

and

Robert H. Titran  
*Lewis Research Center*  
*Cleveland, Ohio*

Prepared for the  
Tenth Symposium on Space Nuclear Power and Propulsion  
sponsored by the Institute for Space Nuclear Power Studies  
Albuquerque, New Mexico, January 10-14, 1993

**NASA**

## PROCESSING AND MICROSTRUCTURE OF Nb-1%Zr-0.1%C ALLOY SHEET

Mehmet Uz  
Lafayette College  
Easton, PA 18042

Robert H. Titran  
NASA Lewis Research Center  
Cleveland, Ohio 44135

### Abstract

A systematic study was carried out to evaluate the effects of processing on the microstructure of a Nb-1wt.%Zr-0.1wt.%C alloy sheet. The samples were fabricated by cold rolling different sheet bars that were single-, double- or triple-extruded at 1900 K. Heat treatment consisted of one- or two-step annealing of different samples at temperatures ranging from 1350 K to 1850 K. The assessment of the effects of processing on microstructure involved characterization of the precipitates including the type, crystal structure, chemistry and distribution within the material as well as an examination of the grain structure. A combination of various analytical and metallographic techniques were used on both the sheet samples and the residue extracted from them. The results show that the relatively coarse orthorhombic Nb<sub>2</sub>C carbides in the as-rolled samples transformed to rather fine cubic monocarbides of Nb and Zr with varying Zr/Nb ratios upon subsequent heat treatment. The relative amount of the cubic carbides and the Zr/Nb ratio increased with increasing number of extrusions prior to cold rolling. Furthermore, the size and the aspect ratio of the grains appear to be strong functions of the processing history of the material. These and other results obtained will be presented with the emphasis on a possible relationship between processing and microstructure.

### INTRODUCTION

Space power requirements for future civil missions, such as exploration of the Moon and Mars, will range from multikilowatts to megawatts of electricity. One of the more important areas presently under investigation concerns the characterization of materials for the primary heat source - a nuclear reactor. The requirements for such a nuclear power system currently include a service life in excess of 7 years at temperatures greater than 1350 K, less than 2% total creep strain under stresses as high as 21 MPa, and resistance to environmental degradation. These criteria dictate the use of refractory metals (Cooper 1984). Refractory metal alloys like Nb-1%Zr (this and all of the following compositions being in wt.%) have been suggested for use in space power applications where resistance to liquid alkali metal corrosion at temperatures near 1100 K is the primary concern (Lane and Ault 1965, Buckman 1984). Preliminary designs of space nuclear power systems for ground demonstration specify the Nb-1%Zr alloy for the reactor vessel, heat pipe, and power components (Kruger et al. 1987). Current concepts need Nb-base alloys with greater high temperature strength and increased creep resistance to provide additional design and safety margins (Dokko et al. 1984) as compared to those provided by Nb-1%Zr alloy. The primary candidates to provide such margins are the carbide-strengthened Nb-alloys, in particular, the so-called PWC-11 developed in the 1960s (DelGrosso et al. 1967) with a nominal composition of Nb-1%Zr-0.1%C. An earlier study (Uz and Titran 1991) showed that a Nb-1%Zr-0.06%C alloy has excellent microstructural stability at temperatures of interest with or without applied load. The total creep strain in a sample of this low-carbon alloy was less than 0.1% after 4 years ( $\approx 35,000$  hours) at 1350 K under a stress of 10 MPa.

There has been substantial work reported on the Nb-1%Zr-C alloys, especially on a Nb-1%Zr alloy containing 0.06%C including its microstructure, long-term creep resistance under different loads, and its weldability (Titran 1986 and 1990, Grobstein and Titran 1986, Titran et al. 1986 and 1987, Moore et al. 1986, Uz and Titran 1991). However, the relationship between processing, microstructure and properties has not been well-established for these alloys.

The present study is part of National Aeronautics and Space Administration (NASA) Lewis Research Center's ongoing program of a critical evaluation of Nb-Zr-C alloys to determine the feasibility of the PWC-11 alloy to meet the anticipated temperature and creep resistance requirements needed to replace the Nb-1%Zr in SP-100 space power systems. It deals with the characterization of the microstructure of a Nb-1 %Zr-

0.1%C alloy sheet as affected by the thermomechanical processing employed in its fabrication and the subsequent heat treatment prior to its use in service. In particular, the paper examines the effects of multiple hot-extrusions prior to cold rolling as well as the effects of various high-temperature anneals on the microstructure.

## EXPERIMENTAL

The Nb-1%Zr-0.1%C alloy was procured commercially as vacuum arc-melted ingot with a heat number of 064, hence the label of each sample in this study consists of the heat number followed by an identification indicative of the process. Table 1 gives the processing history of the samples studied all of which were in the form of 1-mm thick sheet. The difference between each group of samples is that 064A, 064B and 064C were given, respectively, single-, double- and triple-extrusion operations prior to cold-rolling the sheet bar. All the extrusions were made at 1900 K with an extrusion-ratio of 4:1. The samples from 064A were given two sets of heat treatments - one with 1755 K constant and the other with 1475 K constant. This was done to determine the role of each of these temperatures in the double-anneal (DA) heat treatment (1 h at 1755 K + 2 h at 1475 K) recommended for the PWC-11 alloys (Del Grosso, et al. 1967), and the consequences of changing either of these temperatures. Smaller variations in heat treatments were performed on the samples from 064B and 064C in order to determine the effects of the number of extrusions on the microstructure. Heat treatments were carried out at a pressure of the order of  $10^{-7}$  Pa with each specimen wrapped in chemically-cleaned tantalum foil as an additional precaution against interstitial impurity contamination.

TABLE 1. Processing Histories of the 1-mm Thick Sheet Samples from Nb-1%Zr-0.1%C Alloy 064.

SAMPLE	NO. OF EXTRUSIONS	CONDITION OR HEAT TREATMENT
064A	1	AS COLD-ROLLED (96% CW)
064A-1755	1	1h @ 1755K
064A-1755/1350	1	1h @ 1755K + 2h @ 1350K
064A-1755/1475 (064A-DA)	1	1h @ 1755K + 2h @ 1475K
064A-1755/1600	1	1h @ 1755K + 2h @ 1600K
064A-1755/1700	1	1h @ 1755K + 2h @ 1700K
064A-1475/1475	1	1h @ 1475K + 2h @ 1475K
064A-1650/1475	1	1h @ 1650K + 2h @ 1475K
064A-1850/1475	1	1h @ 1850K + 2h @ 1475K
064B	2	AS COLD-ROLLED (88% CW)
064B-1755	2	1h @ 1755K
064B-1755/1350	2	1h @ 1755K + 2h @ 1350K
064B-1755/1475 (064B-DA)	2	1h @ 1755K + 2h @ 1475K
064C <sup>(a)</sup>	3	AS COLD-ROLLED (60% CW)
064C-1755	3	1h @ 1755K
064C-1755/1350	3	1h @ 1755K + 2h @ 1350K
064C-1755/1475 (064C-DA)	3	1h @ 1755K + 2h @ 1475K

<sup>(a)</sup>Also cross-rolled to meet sheet-width requirements.

All the materials were chemically analyzed to verify their initial compositions. The samples exposed to elevated temperatures were also analyzed for O, N and C to monitor their loss or pick up during such exposures because these elements are known to affect material properties significantly.

The longitudinal and transverse cross-sections of each specimen were examined and photographed using light microscopy in the as-polished condition. Mechanical polishing was done in a slurry of 50 ml water - 50 ml colloidal silica with 1 ml each of hydrofluoric and nitric acids on an acid-resistant polishing cloth. The samples were also chemically etched with a solution of lactic acid:nitric acid:hydrofluoric acid in a ratio of 6:3:1 by volume to examine the grain structure. Some specimens were further examined and photographed using scanning electron microscopy (SEM) in the as-polished condition. Thin-film samples of 064A, 064A-DA, 064B-DA and 064C-DA were examined by transmission electron microscopy (TEM) to characterize the size, shape, crystal structure and Zr/Nb ratio of the precipitates.

The microstructure was further characterized by examining the second phase particles extracted from each sample using a solution of 900 ml methanol - 100 ml bromine - 10 g tartaric acid with platinum as a catalyst. Phase-extracted residue from each sample was analyzed by X-ray spectroscopy to determine the crystal structure and lattice parameters, and by inductively-coupled plasma technique (ICP) for Nb- and Zr-contents. Pieces of the filter paper with residue retained from 064A, 064A-DA, 064B-DA, 064C-DA were examined using SEM for appearance, and analyzed for Zr/Nb ratio by energy-dispersive X-ray spectroscopy (XEDS).

The procedure followed in this study was designed to allow microstructural characterization to be done by two or more independent methods. This was done for selected samples to validate the trends established using the results obtained by the techniques common to all of the samples studied.

## RESULTS AND DISCUSSION

### Chemical Analysis

The results of the chemical analyses are tabulated in Table 2 above. It is evident that there has been noticeable oxygen contamination in 064B-1755/1350, and oxygen and nitrogen contaminations in 064C-1755 and 064C-1755/1350 during the heat treatment of these samples. In an earlier study on Nb-1%Zr-0.06%C

TABLE 2. Results of the Chemical Analysis of Samples whose Processing Histories are given in Table 1.

CHEMICAL COMPOSITION (WT.%)					
SAMPLE	O <sup>(a)</sup>	N <sup>(a)</sup>	C <sup>(b)</sup>	Zr <sup>(c)</sup>	Nb
064-INGOT(TOP)	0.0050	0.0025	0.0910	0.96	BALANCE
064-INGOT(BOTTOM)	0.0080	0.0020	0.0900	0.94	
064A	0.0035	0.0025	0.0900	0.93	
064A-1755	0.0018	0.0025	0.0982	0.982	
064A-1755/1350	0.0029	0.0022	0.0972	----	
064A-DA	0.0028	0.0019	0.0921	----	
064A-1755/1600	0.0014	0.0018	0.0965	----	
064A-1755/1700	0.0027	0.0014	0.0957	----	
064A-1475/1475	0.0035	0.0015	0.0982	----	
064A-1650/1475	0.0063	0.0014	0.0979	----	
064A-1850/1475	0.0024	0.0016	0.0943	----	
064B-1755	0.0040	0.0021	0.0970	----	
064B-1755/1350	0.0248	0.0040	0.0974	----	
064B-DA	0.0033	0.0022	0.0914	----	
064C-1755	0.0593	0.0116	0.1040	----	
064C-1755/1350	0.0283	0.0086	0.1020	----	
064C-DA	0.0022	0.0009	0.0944	----	

<sup>(a)</sup>Inert-gas fusion method. <sup>(b)</sup>Combustion extraction method. <sup>(c)</sup>Inductively-coupled plasma method.

alloy (Uz and Titran 1991), the oxygen content in the stressed middle portion of a creep sample increased from about 0.003 wt.% to 0.043 wt.% after 34,500 hours at 1350 K under 10 MPa. This did not affect either the high-temperature creep resistance or microstructural stability of the material which also should be the case for the samples studied here. However, any appreciable interstitial impurity, especially oxygen pick up during processing should be avoided since liquid alkali metals that may be present in the service environment of these materials are much stronger oxide-formers than either Zr or Nb (Kubachewski and Alcock 1983).

### Metallographic Examination of Sheet Samples

The samples were examined using optical microscopy, scanning electron microscopy (SEM) and/or transmission electron microscopy (TEM). These will be presented starting with the as-cast alloy and follow the process path for a group of samples. All the micrographs of the sheet samples presented are from the longitudinal cross-sections, and the direction of cold work (rolling axis) in each is parallel to the horizontal lines of the text with the exception of Figure 2 in which the extrusion axis is nearly perpendicular.

Secondary-electron (SE) images of as-cast 064 taken by SEM are shown at two different magnifications in Figure 1. The needle-like precipitates are rather coarse throughout the matrix and appear to have formed a continuous network along the boundaries of the grains that are relatively large.

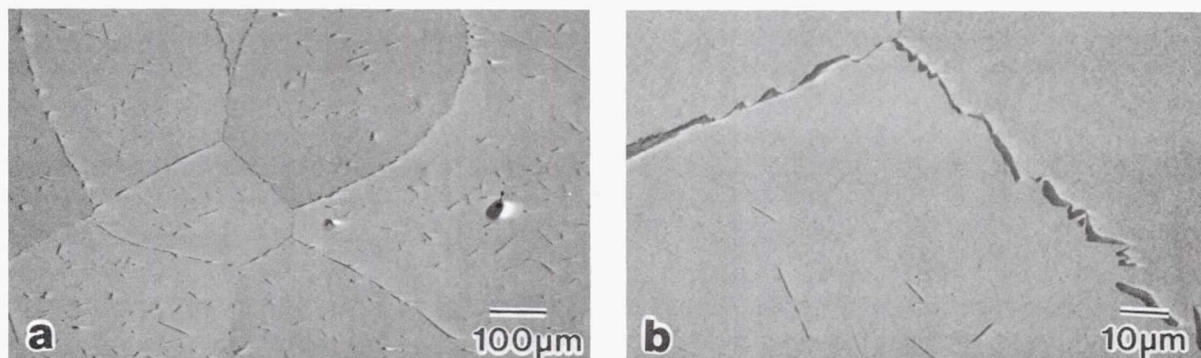


FIGURE 1. SEM Micrographs of As-Cast Nb-1%Zr-0.1%C Alloy 064. Both Secondary Electron Images (SEI) of the Longitudinal Cross Section of As-Etched Sample.

Shown in Figure 2 are the back-scattered electron (BSE) images of the nose portion of the single-extruded sheet bar at two different magnifications. It would appear that hot extrusion at 1900 K caused the as-cast structure to break down and reform with the precipitates somewhat aligned along the direction of deformation. Also, the extrusion process evidently resulted in noticeable refinement in the precipitate size.

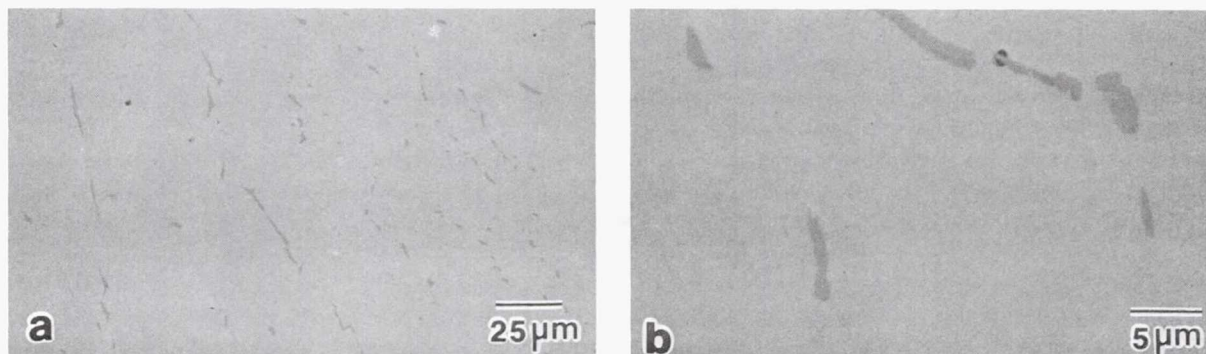


FIGURE 2. SEM Micrographs of Single-Extruded Sheet Bar of Nb-1%Zr-0.1%C Alloy 064. Both Back Scattered Electron Images (BSEI) of the Longitudinal Cross Section of As-Polished Sample.

A complete breakdown of the microstructure and alignment of the mostly coarse precipitates along the rolling direction occurred upon cold rolling following extrusion as can be seen from Figure 3a. The remaining micrographs in the figure show the effects of changing the second-step temperature of the double-anneal heat treatment. Figure 3b shows that there is a refinement of the precipitate size accompanied by the appearance of individual grains upon heating the as-rolled sample for 1 h at 1755 K. Also noteworthy from this micrograph is the presence of the finer precipitates along the grain boundaries as well as within the grains.

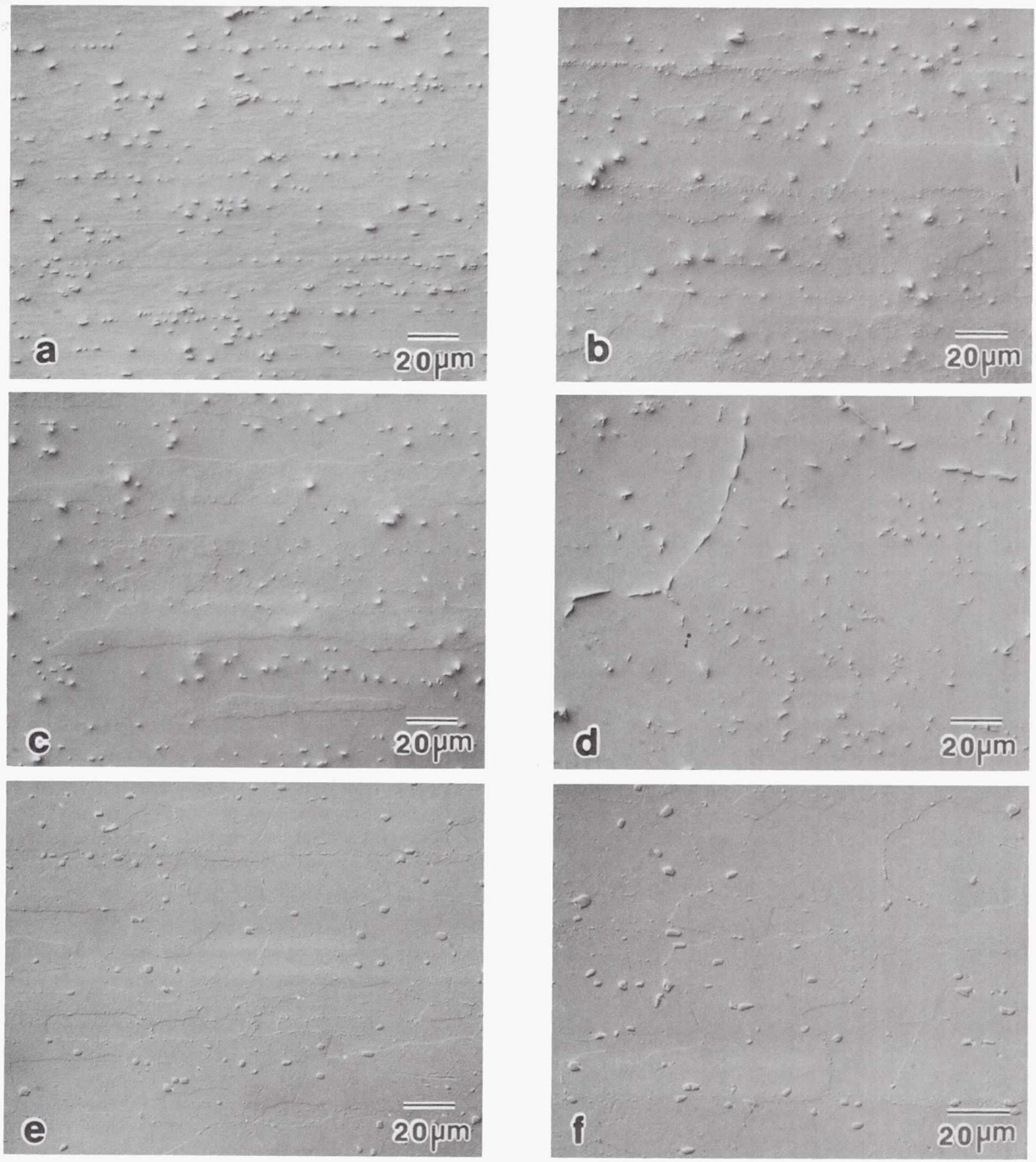


FIGURE 3. Optical Micrographs of (a) 064A, (b) 064A-1755, (c) 064A-1755/1350, (d) 064A-DA, (e) 064A-1755/1600 and (f) 064A-1755/1700. All Differential Interference Contrast (DIC) Images of the Longitudinal Cross Sections of As-Polished Samples.

Subsequent anneal at 1350 K for 2 h caused some coarsening of the precipitates and a slight decrease in the aspect ratio of the grains which can be noted from the optical micrograph of 064A-1755/1350 in Figure 3c. The grains of both 064A-1755 and 064A-1755/1350 are mostly elongated, and few grains have aspect ratios as high as 10 and a length of up to 100  $\mu\text{m}$ . The nearly equiaxed grains in either sample are rather small ( $\approx 10 \mu\text{m}$ ). Upon double-anneal, DA (1 h at 1755 K + 2 h at 1475 K), the sample 064A recrystallized fully as is obvious from the optical micrograph of 064A-DA in Figure 3d. The grains in this sample are rather large (100 to 300  $\mu\text{m}$ ) with relatively coarse precipitates along the grain boundaries and within grains alike. The highest aspect ratio measured in this sample was about 1.5. It is interesting to note from the micrographs of 064A-1755/1600 in 3e and 064A-1755/1700 in 3f that increasing the second-step temperature of DA heat treatment did not result in a coarser microstructure. In contrast to what one would expect, these samples have much finer microstructures than 064A-DA as far as both the grain size and the precipitates are concerned. The coarser precipitates observed in the as-rolled sample are fewer in number, and newly-formed fine precipitates are visible within the grains and the boundaries. It is possible that increasing the second-step temperature hastened the formation of the finer precipitates following the partial solution treatment at 1755 K. These finer precipitates were then responsible for hindering the grain growth, hence the finer microstructure. The larger grains in either of these last two samples are as long as 150  $\mu\text{m}$  with an aspect ratio as high as 5. Again the nearly-equiaxed grains are on the order of 10  $\mu\text{m}$  in size. These heat treatments should be duplicated to further investigate the rather unusual trends in the resulting microstructures.

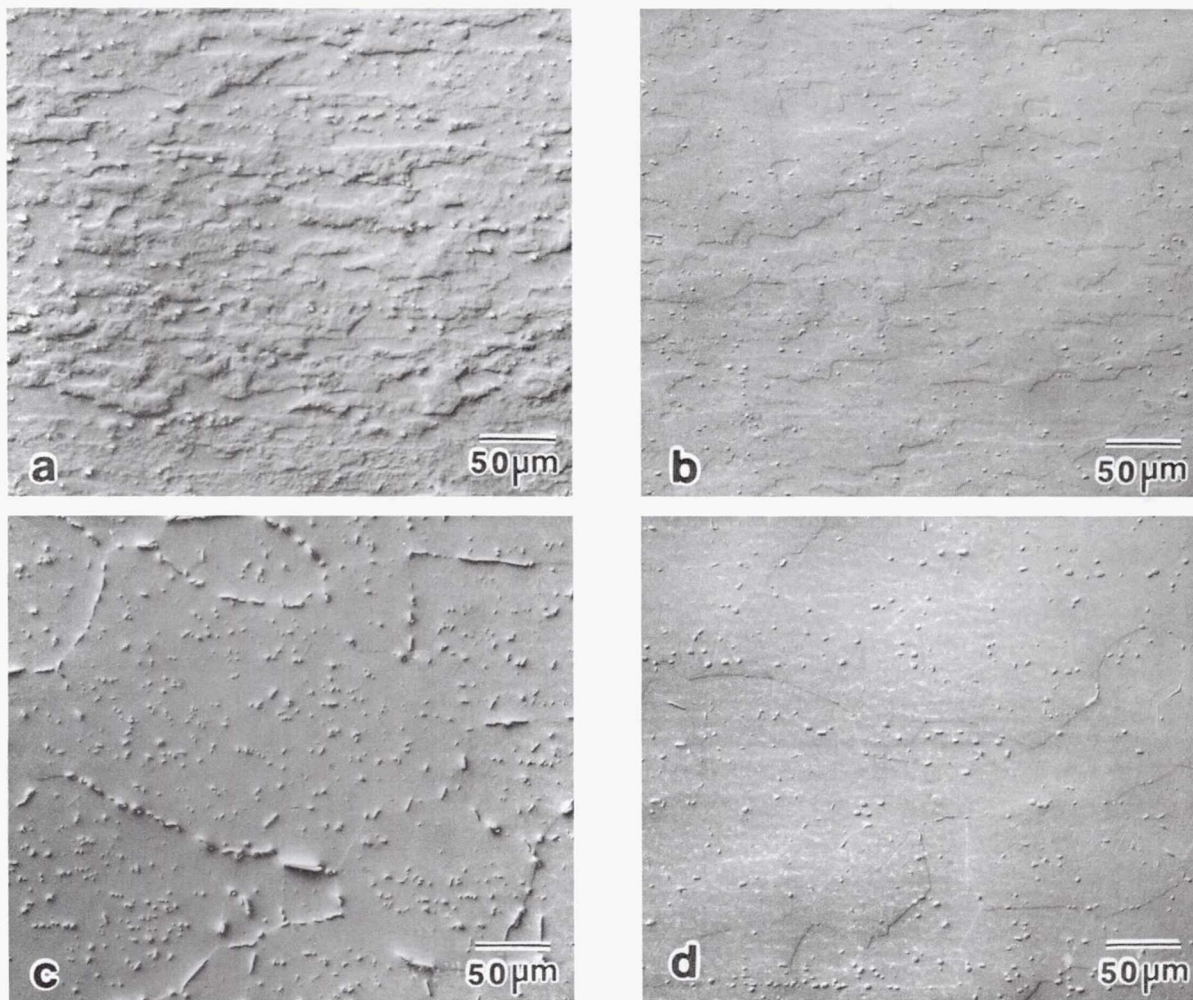


FIGURE 4. Optical Micrographs of (a) 064A-1475/1475, (b) 064A-1650/1475, (c) 064A-DA and (d) 064A-1850/1475. All DIC Images of the Longitudinal Cross Sections of As-Polished Samples.

The development of the microstructure of 064A upon changing the first-step temperature of the DA heat treatment is shown in Figure 4. There appears to be some refinement in the precipitate size upon 1475/1475 anneal (Figure 4a), but this is to a lesser extent than in 064A-1755 above. This should be expected since much less carbon goes into solution at 1475 K than at 1755 K, and consequently less re-precipitates during cooling and/or subsequent heat treatment. Increasing the first-step temperature to 1650 K resulted in a marked refinement of the microstructure (see Figure 4b). Both of the above anneals gave grains as long as 100  $\mu\text{m}$  with aspect ratios as high as 5 to 8. The nearly-equiaxed grains are smaller ( $\approx 5$  to 10  $\mu\text{m}$ ) than the samples discussed previously. The DA heat treatment resulted in a coarse recrystallized microstructure as described earlier. Interesting again is that increasing the first-step temperature to 1850 K (sample 064A-1850/1475 in Figure 4.d) yielded a finer microstructure than 064A-DA. The grains have aspect ratios of 1 to 2. The equiaxed grains are as small as 30  $\mu\text{m}$ , and the elongated ones are as long as 150  $\mu\text{m}$ . Both the grains and the precipitates in this sample are considerably finer than those in 064A-DA. This may be attributable to more carbon going into solution at 1850 K than at 1755 K, and more carbon being available for the formation of the finer carbides in the sample annealed at the higher temperature. These stable precipitates then prevented grain growth.

The microstructures of the as-rolled and heat treated samples from the double-extruded sheet 064B are shown in Figure 5. The trends concerning the changes in the microstructure are similar to those observed in samples from 064A (see Fig. 3a - 3d). There is some refinement in the microstructure upon annealing of

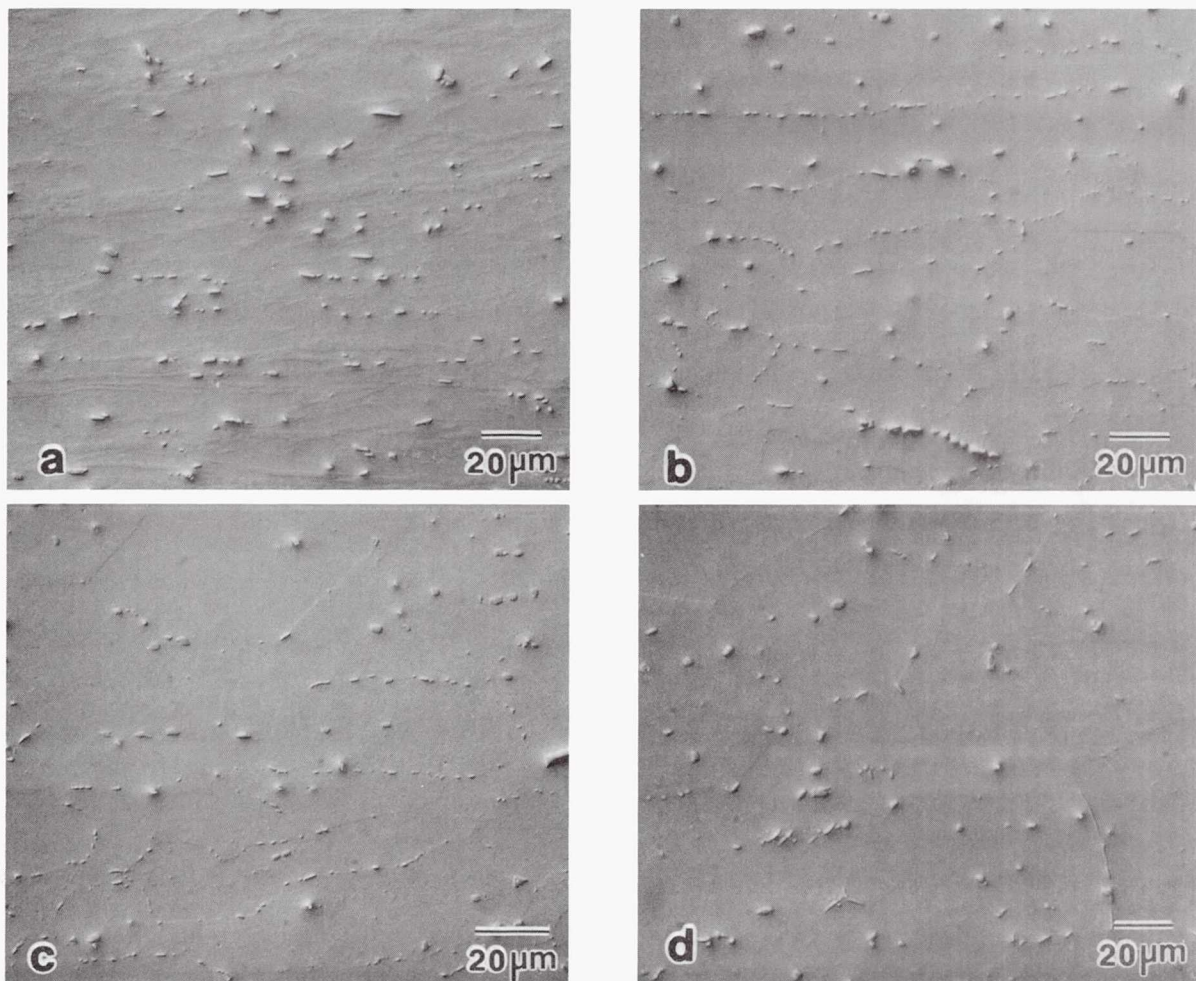


FIGURE 5. Optical Micrographs of (a) 064B, (b) 064B-1755, (c) 064B-1755/1350, (d) 064B-DA. All DIC Images of the Longitudinal Cross Sections of As-Polished Samples.

the cold-rolled sample at 1755 K for 1 h, and upon the subsequent anneal of 2 h at 1350 K. The grains of 064B-1755 are mostly elongated (as long as 150  $\mu\text{m}$ ) and have aspect ratios as high as 10. A few of the grains appear to be nearly equiaxed and are about 20  $\mu\text{m}$  in size. The microstructure of 064B-1755/1350 appears similar, but the grains have lower aspect ratios with a maximum of about 6. Similar to that of 064A-DA, the microstructure of 064B-DA is almost fully recrystallized, but with smaller grains and finer precipitates that appear to be less in number density. This may be attributed to the lower amount of cold work in 064B ( $\approx 88\%$ ) than that in 064A ( $\approx 96\%$ ) which means lower stored energy hence less driving force for the recrystallization and growth processes. Furthermore the grains in 064B-DA are considerably finer than in 064A-DA and some still have an aspect ratio as high as 3.

Figure 6 shows the optical micrographs of the samples from the triple-extruded 064C which were similarly processed as those from 064B in Figure 5. It appears that the precipitates in these samples from 064C are finer than the similarly-treated samples from either 064A or 064B. It will be recalled that 064C received only 60% cold work which is much less than the other two, but it was cross-rolled to meet the width requirements during the sheet manufacturing process (Table 1). This more complex (than straight rolling) process evidently more than made up for the lower percent of cold work it received. It is interesting to note from Figure 6d that, in contrast to 064A-DA and 064B-DA, 064C-DA is not recrystallized. The grains of 064C-DA are noticeably finer than either of the other two, and have aspect ratios as high as 8 to 10. This may be due to the fine precipitates at the grain boundaries, or due to some stabilizing effect of the cross-rolling process.

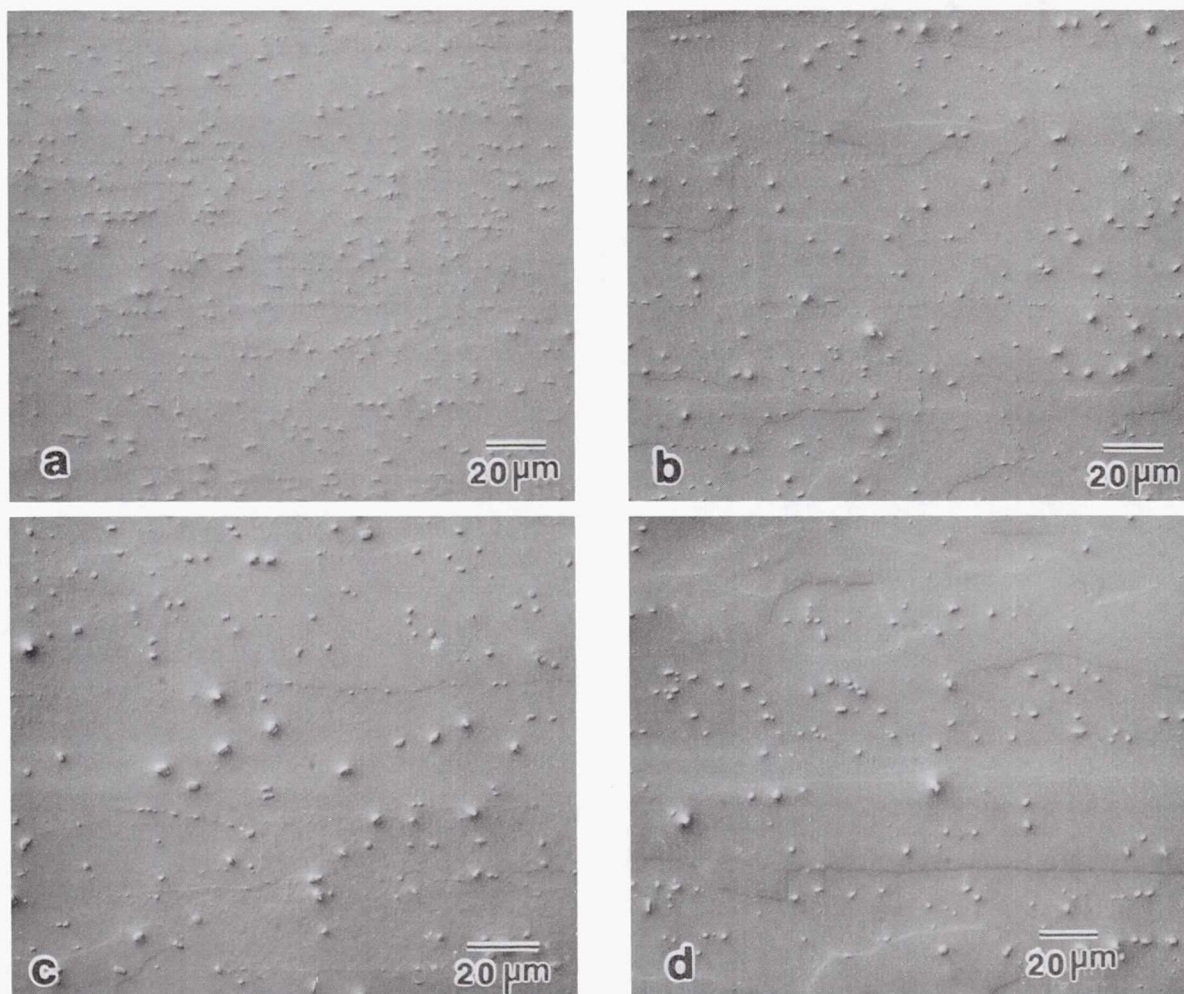


FIGURE 6. Optical Micrographs of (a) 064C, (b) 064C-1755, (c) 064C-1755/1350, (d) 064C-DA. All DIC Images of the Longitudinal Cross Sections of As-Polished Samples.

The back-scattered electron images of some of the samples examined using SEM are shown in Figure 7. These micrographs correlate well with the optical images concerning the precipitates - the carbides which have a lower average atomic number than the matrix appear darker in the BSE images and correspond to the protrusions in the micrographs taken by light microscope using differential interference contrast (DIC). Furthermore, these micrographs show that the precipitates in the heat-treated samples vary in size from the fraction of a micron to a few microns. The larger precipitates, however, appear to be fewer in number, especially in the sample from the triple-extruded sheet.

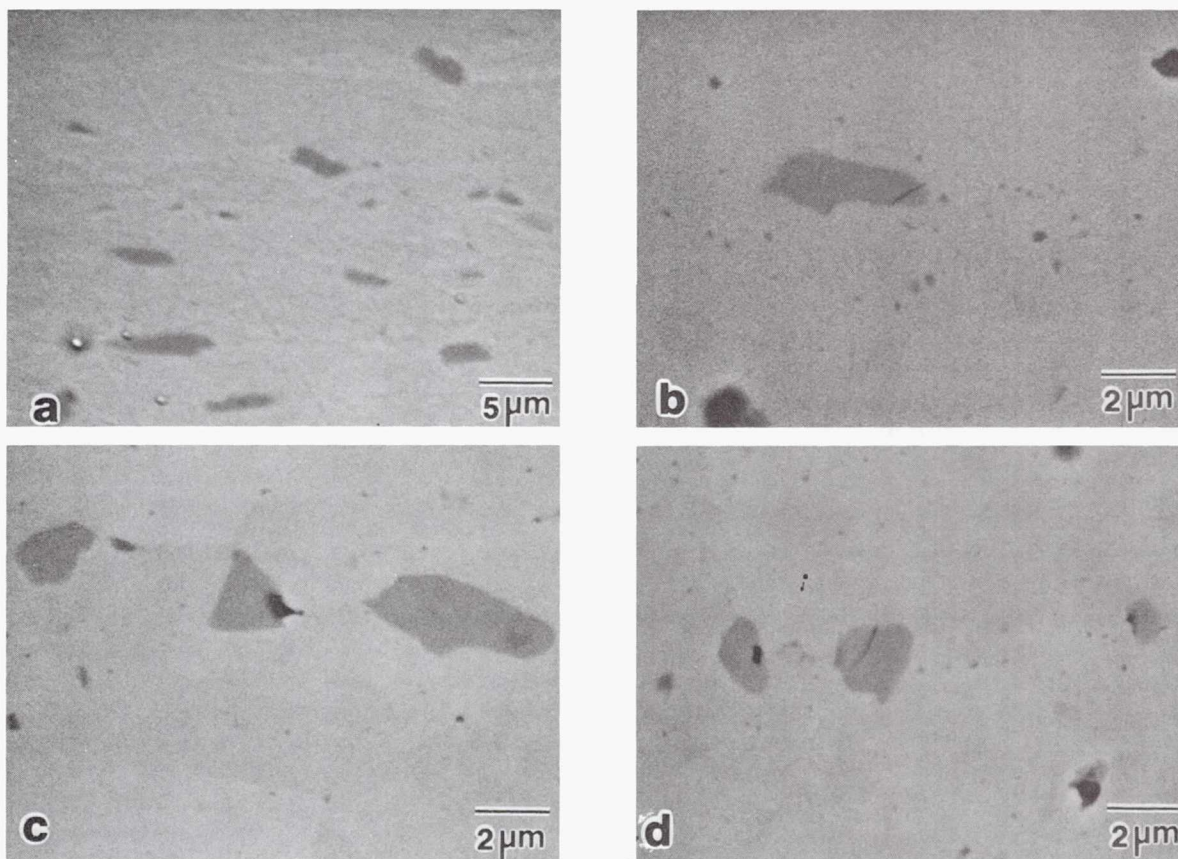


FIGURE 7. SEM Micrographs of (a) 064A, (b) 064A-1755, (c) 064A-1755/1350, (d) 064C-1755/1350. All BSEI of the Longitudinal Cross Sections of As-Polished Samples.

The above results show that it is possible to obtain different microstructures as desired by carefully tailoring the process. With the exceptions of 064A-DA, 064A-1850/1475 and 064B-DA, all the processes resulted in microstructures consisting of relatively fine precipitates along the grain boundaries and within the grains, but the grains themselves had preferred orientation and widely varying aspect ratios. Relative to one with equiaxed grains, such microstructures with elongated grains may be beneficial in improving the mechanical properties in the longitudinal direction, but would be detrimental for those in the transverse direction.

#### Characterization of Precipitates

The precipitates that may form individually or in solid solution with one another in a Nb-Zr-C alloy are listed in Table 3 together with the crystal structure and lattice parameters. To identify and characterize the precipitates in the samples examined, phase-extracted residue from each was analyzed following the procedure described earlier. For the same purpose, and also to verify the results obtained from X-ray analysis, some sheet samples were examined and analyzed using TEM to identify the precipitates and to determine their

**TABLE 3: Crystal structures and lattice parameters of compounds possibly present in Nb-Zr-C alloys.**

Compound	Crystal Structure	Lattice Parameter (nm)		
		$a_0$	$b_0$	$c_0$
Nb <sub>2</sub> C	Hexagonal	0.313	----	0.497
Nb <sub>2</sub> C	Orthorhombic	1.09	0.31	0.50
NbO	Cubic	0.421	----	----
NbN	Tetragonal	0.438	----	0.431
NbN	Hexagonal	0.295	----	0.553
NbC	fcc(B1)	-->0.447	----	----
ZrN	fcc(B1)	0.456	----	----
ZrO	fcc(B1)	0.462	----	----
ZrC	fcc(B1)	-->0.470	----	----
ZrO <sub>2</sub>	fcc(C1)	0.509	----	----

crystal structures, lattice parameters and chemistry. It is realized that the error involved in XEDS analysis using SEM or TEM can be as high as 20% relative to the value measured. However, independent techniques on select samples are useful in verifying the trends observed in the results obtained from the analysis techniques, such as ICP and X-ray spectroscopy, common to all samples studied.

Figure 8 shows the SEM images of the residue samples gathered on filter paper from (a) 064A, (b) 064B-DA. It will be noted that in the residue from 064A the individual particles can be resolved while those in the other agglomerated together indicating that they are finer overall which is consistent with the metallographic observations discussed earlier. Residue from other heat-treated samples looked similar to that of 064B-DA.

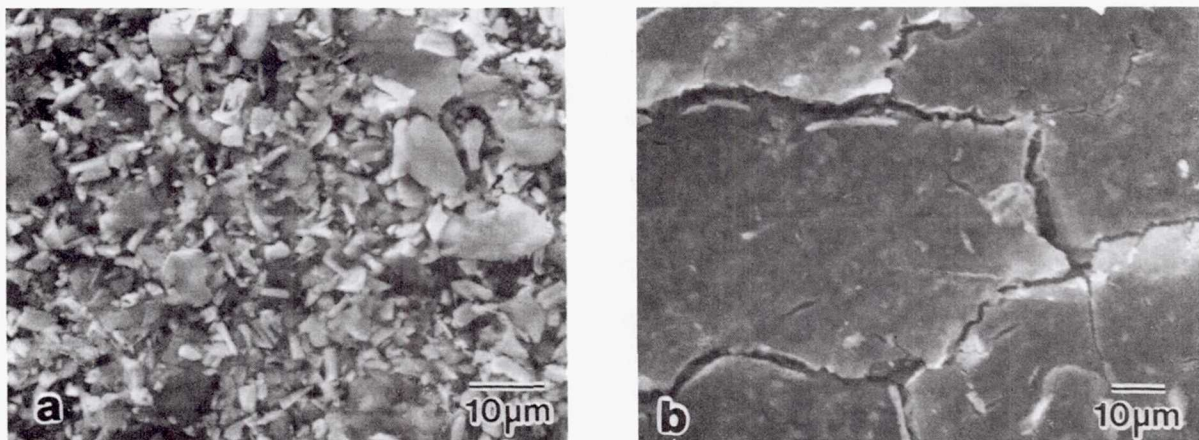


**FIGURE 8. SEM Micrographs of the Residue extracted from (a) 064A and (b) 064B-DA. Both SEI of the Residue gathered on Teflon Filter Paper.**

The results of the analysis of the phase extracted residue by X-rays, ICP technique and SEM/XEDS are tabulated in Table 4. Given in Table 5 are the results of TEM work on thin-film samples from 064A, 064A-DA, 064B-DA, 064C-DA. The results in Table 5 concerning the precipitate identity and the lattice parameters that could be determined are consistent with those in Table 4 for these specimens. TEM images of precipitates of two different sizes are shown in Figure 9 together with the corresponding diffraction pattern of each.

TABLE 4: Results of the analysis of residues phase-extracted from Nb-1%Zr-0.1%C alloy samples whose processing histories are given in Table 1.

SAMPLE	X-RAY ANALYSIS				Zr/Nb RATIO	
	PHASE(S)	LATTICE PARAMETERS (nm)			CHEM ANALYSIS	SEM <sup>(a)</sup> XEDS
		a <sub>0</sub>	b <sub>0</sub>	c <sub>0</sub>		
064A-INGOT	Nb <sub>2</sub> C	(b)			2/98	
064A	Nb <sub>2</sub> C	1.092	0.497	0.311	3/97	10/90
	(Zr,Nb)C	0.453				
064A-1755	(Zr,Nb)C	(b)			26/74	
064A-1755/1350	(Nb,Zr) <sub>2</sub> C	1.239	1.093	0.499	15/85	
	(Zr,Nb)C	0.452				
064A-DA	Nb <sub>2</sub> C	1.090	0.480	0.290	10/90	
	(Zr,Nb)C	0.450				30/70
064A-1755/1600	(Nb,Zr) <sub>2</sub> C	1.239	1.093	0.498	20/80	
	(Zr,Nb)C	0.452-				
		0.459				
064A-1755/1700	(Nb,Zr) <sub>2</sub> C	1.241	1.090	0.498	10/90	
	(Zr,Nb)C	0.452				
064A-1475/1475	(Nb,Zr) <sub>2</sub> C	1.236	1.086	0.497	20/80	
	(Zr,Nb)C	0.454				
064A-1650/1475	(Nb,Zr) <sub>2</sub> C	1.236	1.088	0.497	20/80	
	Zr,Nb)C	0.456				
064A-1850/1475	(Nb,Zr) <sub>2</sub> C	1.239	1.090	0.498	4/96	
064B	Nb <sub>2</sub> C	1.090	0.499	0.311	15/85	
	(Zr,Nb)C	(b)				
064B-1755 <sup>(c)</sup>	(Nb,Zr) <sub>2</sub> C	1.240	1.089	0.497	20/80	
	(Zr,Nb)C	0.459				
064B-1755/1350 <sup>(c)</sup>	(Nb,Zr) <sub>2</sub> C	(b)			20/80	
	(Zr,Nb)C	0.459				
064B-DA	Nb <sub>2</sub> C	(b)			40/60	50/50
	(Zr,Nb)C	0.459				
064C	Nb <sub>2</sub> C	1.090	0.497	0.311	25/75	
	(Zr,Nb)C	(b)				
064C-1755 <sup>(c)</sup>	(Nb,Zr) <sub>2</sub> C	1.238	1.090	0.498	30/70	
	(Zr,Nb)C	0.461				
064C-1755/1350 <sup>(c)</sup>	(Nb,Zr) <sub>2</sub> C	(b)			50/50	
	(Zr,Nb)C	0.459				
064C-DA	(Zr,Nb)C	0.459			65/35	70/30

(a) Average of XEDS analysis of 4 areas from 5x5 μm to 250x250 μm.

(b) Not enough peaks to determine lattice parameters.

(c) In these samples some ZrO<sub>2</sub> was also detected.

It will be noted from Table 5 that the finer (submicron-sized) particles are predominantly cubic (Zr,Nb)C with relatively high Zr/Nb ratios whereas the coarser ones (3-5 μm in size) are orthorhombic Nb<sub>2</sub>C with quite low Zr/Nb ratios. This indicates that as the Zr/Nb ratio increases, the fraction of the precipitates that are cubic (Zr,Nb)C, i.e. the relative amount of these precipitates in a material increases. This should be desirable as the finer cubic alloy carbide is more stable than the coarser Nb<sub>2</sub>C. In fact, Nb<sub>2</sub>C dissolves with time giving

TABLE 5: Results of TEM studies on thin-films of Nb-1%Zr-0.1%C alloy sheet samples

SAMPLE	PRECIPITATE		LATTICE PARAMETER ( $\mu\text{m}$ )			Zr/Nb
	SIZE( $\mu\text{m}$ )	TYPE	$a_0$	$b_0$	$c_0$	
064A	0.1x0.3	Nb <sub>2</sub> C	----	----	----	4/96
	0.25x0.25	Nb <sub>2</sub> C	----	----	----	3/97
064A-DA	4	Nb <sub>2</sub> C	1.092	----	----	2/98
	4	Nb <sub>2</sub> C	----	----	----	2/98
	2.5	Nb <sub>2</sub> C	1.092	----	----	5/95
	0.3	(Zr,Nb)C	0.468 <sup>(a)</sup>	----	----	45/55
	0.2x0.3	(Zr,Nb)C	0.461	----	----	40/60
	0.3x0.4	(Zr,Nb)C	0.458	----	----	40/60
	0.2x0.3	(Zr,Nb)C	0.466	----	----	35/65
064B-DA	4	Nb <sub>2</sub> C	1.092 <sup>(b)</sup>	----	----	2/98
	4x5	Nb <sub>2</sub> C <sup>(c)</sup>	0.268	----	----	5/95
	5	Nb <sub>2</sub> C <sup>(c)</sup>	----	----	----	2/98
064C-DA	2x3	Nb <sub>2</sub> C	1.092	----	----	2/98
	2	Nb <sub>2</sub> C	1.092	----	----	2/98
	3	Nb <sub>2</sub> C	----	----	0.309	6/94
	2x4	Nb <sub>2</sub> C	1.092	----	----	5/95
	0.2x0.3	(Zr,Nb)C	0.472	----	----	

<sup>(a)</sup> See Figure 9a.

<sup>(b)</sup> See Figure 9b.

<sup>(c)</sup> These precipitates were hexagonal while all other Nb<sub>2</sub>C were orthorombic. (Zr,Nb)C were cubic.

way to the fine cubic phase, (Zr,Nb)C, and it is the cubic carbides that provide excellent microstructural stability and creep resistance of these alloys at elevated temperatures as was shown for a Nb-1%Zr-0.06%C alloy in an earlier study (Uz and Titran 1991).

From the results obtained on the phase-extracted residue (see Table 4), the following are evident:

- The precipitates in both the as-cast ingot and the single-extruded sheet 064A were virtually all coarse Nb<sub>2</sub>C, hence their analyses yielded nearly all Nb indicating that Zr was in solid solution with Nb.
- In all the heat treated samples from 064A, with the exception of 064A-1850/1475, there was an increase in the Zr/Nb ratio signaling an increase in the relative amount of the (Zr,Nb)C. The residue from 064A-1850/1475 yielded nearly all Nb and the X-ray results yielded an orthorhombic phase with lattice parameters larger than those of Nb<sub>2</sub>C which is thought to be (Nb,Zr)<sub>2</sub>C.
- A comparison of the samples from 064A, 064B and 064C with similar heat treatments clearly shows that the Zr/Nb ratio hence the relative amount of (Zr,Nb)C increased with the number of extrusions. For example, the Zr/Nb ratio increased from about 3/97 in 064A to 15/85 in 064B and to 25/75 in 064C. Also, the Zr/Nb ratio was about 10/90 in 064A-DA, 40/60 in 064B-DA and it was about 60/40 in 064C-DA. This trend was also confirmed by the XEDS analysis of the residue on filter paper made using SEM as can be seen from the table.
- As in 064A, the results of 064B and especially those of 064C show that the heat treatment of the as-rolled sheet gave rise to a marked increase in Zr/Nb ratio, again indicating an increase in the amount of (Zr,Nb)C relative to Nb<sub>2</sub>C. In all three types of samples studied here, double annealing resulted in 2-3 fold increase in the Zr/Nb ratio with respect to the as-rolled material.

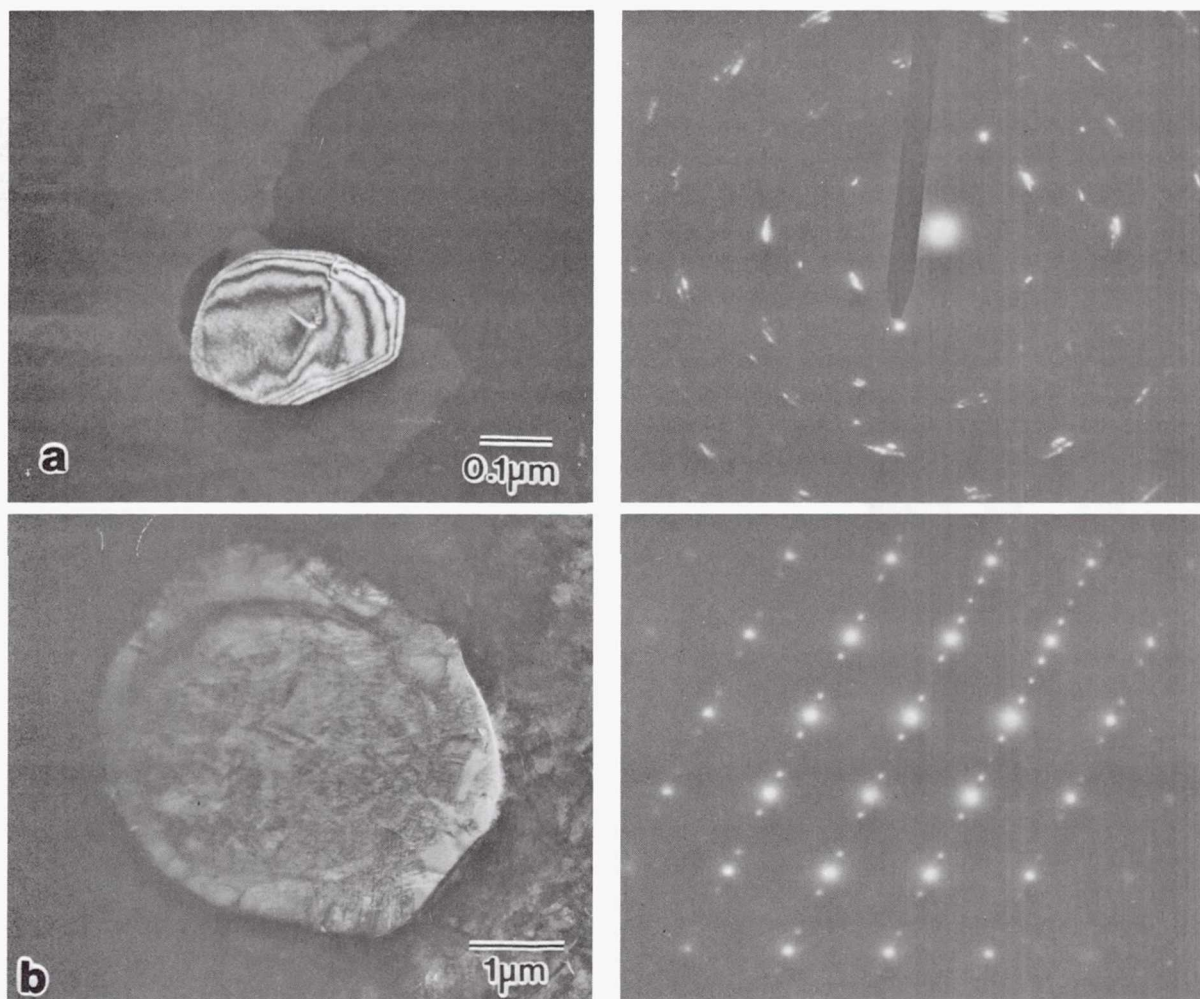


FIGURE 9. TEM Micrographs and the corresponding Diffraction Pattern for (a) a Small ( $\approx 0.3 \mu\text{m}$ ) Particle from 064A-DA and (b) a Large ( $\approx 4 \mu\text{m}$ ) Particle from 064B-DA.

The reasoning behind the identification of some of the orthorhombic carbides in Table 4 as  $(\text{Nb,Zr})_2\text{C}$  and the cubic monocarbides as  $(\text{Zr,Nb})\text{C}$  is as follows:  $\text{Nb}_2\text{C}$  is primarily orthorhombic with  $a_0=1.092 \text{ nm}$ ,  $b_0=0.4974 \text{ nm}$  and  $c_0=0.309 \text{ nm}$  (see Table 3). Also, Zr has a larger atomic radius (0.158 nm) than Nb (0.143 nm). Therefore, as any Zr dissolves in  $\text{Nb}_2\text{C}$ , one would expect an increase in the lattice parameter of this orthorhombic carbide. Currently, the existence of  $(\text{Nb,Zr})_2\text{C}$  is conjectural and solely based on the above because there is no data available concerning  $\text{Zr}_2\text{C}$ . As for the monocarbides, all of them have lattice parameters that fall between those of  $\text{NbC}$  ( $a_0=0.447 \text{ nm}$ ) and  $\text{ZrC}$  ( $a_0=0.470 \text{ nm}$ ). Hence, the cubic precipitates are believed to be a solid solution of  $\text{ZrC}$  and  $\text{NbC}$  or  $(\text{Zr,Nb})\text{C}$ . The increase in the lattice parameter of this precipitate with increasing Zr/Nb ratio also is in agreement with the fact that the lattice parameter of  $\text{ZrC}$  is larger than that of  $\text{NbC}$ . In a material with  $\text{Nb}_2\text{C}$ , formation of  $(\text{Zr,Nb})\text{C}$  or a solid solution of  $\text{ZrC}$  and  $\text{NbC}$  upon exposure to elevated temperatures is thermodynamically possible because  $\text{ZrC}$  is more stable than  $\text{NbC}$  at the temperatures of interest (Kubachewski and Alcock 1983).

The suggestion that some of the relatively coarse  $\text{Nb}_2\text{C}$  dissolves and re-forms as the cubic  $(\text{Zr,Nb})\text{C}$  upon heat treatment is consistent with the results of this study. As processing became more complex or the heat treatment temperature increased, the microstructure showed fewer of the coarser particles and more of the finer ones, and the composition analysis showed an increase in Zr/Nb ratio of the precipitates. This is also consistent with the results of the study on a Nb-1%Zr-0.06%C alloy (Uz and Titran 1991) in which the

microstructure of a sample transformed from one with predominantly Nb<sub>2</sub>C to one with (Zr,Nb)C precipitates in the earlier stages of high-temperature exposure with or without applied load as mentioned earlier.

The results obtained and the observations made in this study show that any of the samples from 064 should be as creep-resistant as the lower-carbon alloy under similar or more severe service conditions. The assessment of the mechanical properties and the processing-microstructure-property relationship for the samples from the Nb-1%Zr-0.1%C alloy are parts of an ongoing investigation.

### SUMMARY OF RESULTS

The effects of processing (number of hot-extrusions prior to cold rolling and subsequent heat treatments) on the microstructure of a Nb-1%Zr-0.1%C alloy was investigated. From the results obtained the following are evident:

- The precipitates present in the alloy are the relatively coarse orthorhombic Nb<sub>2</sub>C with or without Zr dissolved in it and/or the much finer cubic (Zr,Nb)C. Of these precipitates, the cubic carbides are stable and are considered to be responsible for the excellent high-temperature stability and creep resistance of Nb-Zr-C alloys.
- An increase in the Zr/Nb ratio of the extracted carbides corresponds to an increase in the relative amount of the finer cubic carbides in the material which is often accompanied by a finer microstructure.
- With the exceptions of 064A-DA, 064A-1850/1475 and 064B-DA that were almost fully recrystallized, all the processes resulted in microstructures consisting of relatively fine precipitates along the grain boundaries and within the grains, but the grains themselves had preferred orientation and widely varying aspect ratios.
- Comparison of samples with similar heat treatments from the single-, double- and triple-extruded sheets show that the Zr/Nb ratio hence the amount of (Zr,Nb)C in the alloy increased with the number of extrusions prior to cold rolling process. This increase was also accompanied by a finer microstructure and grains of higher aspect ratio.
- In a given group of samples (single-, double- or triple-extruded), all of the heat treatments, in general, resulted in an increase in the Zr/Nb ratio compared to the as-extruded or as-rolled samples.

### CONCLUSION

Based on the results of the earlier study (Uz and Titran 1991) on a Nb-1%Zr-0.06%C alloy which showed excellent creep resistance and microstructural stability at 1350 K, and an examination of the microstructure of the Nb-1%Zr-0.1%C alloy in this study, it would appear that the majority of the samples with the heat-treated conditions from the alloy containing 0.1%C should have as good, if not better, high-temperature stability and creep resistance than those from the lower-carbon alloy even under more severe service conditions.

### Acknowledgements

This work was performed by the NASA Lewis Research Center for the U.S. DOE Office of Nuclear Energy and the Strategic Defense Initiative Office under interagency agreement DE-AI03-86SF16310.

### References

Buckman, R. W. Jr. (1984) in Refractory Alloy Technology for Space Nuclear Applications, R. H. Cooper, Jr. and E. E. Hoffman, eds., CONF-8308130, pp. 86-97, US Department of Energy, Washington, DC.

Cooper, R. H., Jr. (1984) "Potential Refractory Alloy Requirements for Space Nuclear Power Applications," in Refractory Alloy Technology for Space Nuclear Power Applications, R. M. Cooper and E. E. Hoffman, eds., CONF-8308130, pp. 14-17. US Department of Energy, Washington, DC.

DelGrosso, E. J., C. E. Carlson and J. J. Kaminsky (1967) "Development of Niobium-Zirconium-Carbon Alloys," J. Less-Common Metals, 12:173-201.

Dokko, W. et al. (1984) "Applications for Composites and Beryllium in The SP-100 Power System," JPL D-1948, Jet Propulsion Laboratory, Pasadena, CA.

Grobstein, T. L. and R. H. Titran (1986) "Characterization of Precipitates in a Niobium-Zirconium-Carbon-Alloy," NASA TM-100848, NASA Lewis Research Center, Cleveland, OH.

Kruger, G. C., S. Vaidyanathan, N. Deane, R. Protsik and R. E. Murata (1989) "SP-100 Reactor Design," in 22nd Intersociety Energy Conversion Engineering Conference, AIAA, 1:419-423, New York, NY.

Kubachewski, O. and Alcock, C. B.: Metallurgical Thermochemistry, 5th. ed., Pergamon, New York, NY, 1983.

Lane, J. R. and G. M. Ault, (1965) Met. Eng. Q., 5:23-29.

Moore, T. J., R. H. Titran and T. L. Grobstein (1986) "The Effect of Electron Beam Welding on The Creep-Rupture Properties of Nb-Zr-C Alloy," NASA TM-88892, NASA Lewis Research Center, Cleveland, OH.

Titran, R. H. (1986) "Long-Time Creep Behavior of Nb-1Zr Alloy Containing Carbon," NASA TM-100142, NASA Lewis Research Center, Cleveland, OH.

Titran, R. H. (1990) "Creep Strength of Niobium Alloys, Nb-1Zr and PWC-11," NASA TM-102390, Nasa Lewis Research Center, Cleveland, OH.

Titran, R. H., T. J. Moore and T. L. Grobstein (1986) "Creep Properties of PWC-11 Base Metal and Weldments as Affected by Heat Treatment," NASA TM-88842, Nasa Lewis Research Center, Cleveland, OH.

Titran, R. H., T. J. Moore and T. L. Grobstein (1987) "Creep Behavior of Niobium Alloy PWC-11," NASA TM-89834, Nasa Lewis Research Center, Cleveland, OH.

Uz, Mehmet and R. H. Titran (1991) "Thermal Stability of the Microstructure of an Aged Nb-Zr-C Alloy," NASA TM-103647, Nasa Lewis Research Center, Cleveland, OH.

# REPORT DOCUMENTATION PAGE

Form Approved  
OMB No. 0704-0188

Public reporting burden for this collection of information is estimated to average 1 hour per response, including the time for reviewing instructions, searching existing data sources, gathering and maintaining the data needed, and completing and reviewing the collection of information. Send comments regarding this burden estimate or any other aspect of this collection of information, including suggestions for reducing this burden, to Washington Headquarters Services, Directorate for Information Operations and Reports, 1215 Jefferson Davis Highway, Suite 1204, Arlington, VA 22202-4302, and to the Office of Management and Budget, Paperwork Reduction Project (0704-0188), Washington, DC 20503.

<b>1. AGENCY USE ONLY</b> (Leave blank)	<b>2. REPORT DATE</b> October 1992	<b>3. REPORT TYPE AND DATES COVERED</b> Technical Memorandum	
<b>4. TITLE AND SUBTITLE</b>  Processing and Microstructure of Nb-1%Zr-0.1%C Alloy Sheet		<b>5. FUNDING NUMBERS</b>  WU-590-13-11	
<b>6. AUTHOR(S)</b>  Mehmet Uz, Robert H. Titran		<b>8. PERFORMING ORGANIZATION REPORT NUMBER</b>  E-7414	
<b>7. PERFORMING ORGANIZATION NAME(S) AND ADDRESS(ES)</b>  National Aeronautics and Space Administration Lewis Research Center Cleveland, Ohio 44135-3191		<b>10. SPONSORING/MONITORING AGENCY REPORT NUMBER</b>  NASA TM-105921	
<b>9. SPONSORING/MONITORING AGENCY NAMES(S) AND ADDRESS(ES)</b>  National Aeronautics and Space Administration Washington, D.C. 20546-0001		<b>11. SUPPLEMENTARY NOTES</b> Prepared for the Tenth Symposium on Space Nuclear Power and Propulsion sponsored by the Institute for Space Nuclear Power Studies, Albuquerque, New Mexico, January 10-14, 1993.	
<b>12a. DISTRIBUTION/AVAILABILITY STATEMENT</b>  Unclassified - Unlimited Subject Category		<b>12b. DISTRIBUTION CODE</b>	
<b>13. ABSTRACT</b> (Maximum 200 words)  A systematic study was carried out to evaluate the effects of processing on the microstructure of Nb-1wt.%Zr-0.1wt%C alloy sheet. The samples were fabricated by cold rolling different sheet bars that were single-, double- or triple-extruded at 1900 K. Heat treatment consisted of one- or two-step annealing of different samples at temperatures ranging from 1350 K to 1850 K. The assessment of the effects of processing on microstructure involved characterization of the precipitates including the type, crystal structure, chemistry and distribution within the material as well as an examination of the grain structure. A combination of various analytical and metallographic techniques were used on both the sheet samples and the residue extracted from them. The results show that the relatively coarse orthorhombic Nb <sub>2</sub> C carbides in the as-rolled samples transformed to rather fine cubic monocarbides of Nb and Zr with varying Zr/Nb ratios upon subsequent heat treatment. The relative amount of the cubic carbides and the Zr/Nb ratio increased with increasing number of extrusions prior to cold rolling. Furthermore, the size and the aspect ratio of the grains appear to be strong functions of the processing history of the material. These and other results obtained will be presented with the emphasis on a possible relationship between processing and microstructure.			
<b>14. SUBJECT TERMS</b>		<b>15. NUMBER OF PAGES</b> 16	
<b>17. SECURITY CLASSIFICATION OF REPORT</b> Unclassified		<b>16. PRICE CODE</b> A03	
<b>18. SECURITY CLASSIFICATION OF THIS PAGE</b> Unclassified	<b>19. SECURITY CLASSIFICATION OF ABSTRACT</b> Unclassified	<b>20. LIMITATION OF ABSTRACT</b>	

National Aeronautics and  
Space Administration

**Lewis Research Center**  
Cleveland, Ohio 44135

Official Business  
Penalty for Private Use \$300

**FOURTH CLASS MAIL**

**ADDRESS CORRECTION REQUESTED**



Postage and Fees Paid  
National Aeronautics and  
Space Administration  
NASA 451

**NASA**

---